ALCHEMY Jurnal Penelitian Kimia

Official Website: https://jurnal.uns.ac.id/alchemy

ISSN 1412-4092
EISSN 2443-4183

Implementation of FTIR-Based Fingerprinting, Antioxidant Compounds Profiling by UHPLC-Q-Orbitrap HRMS, and Docking Study COVID-19 Inhibitor of Buas-Buas *(Premna serratifolia)* Leaf Extract from Pontianak Indonesia

Dini Hadiarti[a*], Mahwar Qurbaniah[b], Ely Setiawan[c], Taufan Hari Sugara[d]

[a]*Department of Chemical Education, Faculty of Teacher Training and Education, Universitas Muhammadiyah Pontianak*
Jalan Jendal Ahmad Yani No. 111, Pontianak Tenggara, Kota Pontianak, West Kalimantan 78123, Indonesia
[b]*Department of Biological Education, Faculty of Teacher Training and Education, Universitas Muhammadiyah Pontianak*
Jalan Jendal Ahmad Yani No. 111, Pontianak Tenggara, Kota Pontianak, West Kalimantan 78123, Indonesia
[c]*Department of Chemistry, Universitas Jenderal Soedirman*
Jalan Profesor DR. HR Boenyamin No.708, Purwokerto Utara, Banyumas, Central Java 53122, Indonesia
[d]*Department of Pharmacy, Faculty of Health Sciences, Universitas Muhammadiyah Mataram*
Jalan KH. Ahmad Dahlan No.1, Mataram, Kota Mataram, West Nusa Tenggara 83115, Indonesia

[*]*Corresponding author: dinihadiarti@unmuhpnk.ac.id*

DOI: 10.20961/alchemy.21.1.92020.149-161

Received 10 August 2024, Revised 14 December 2024, Accepted 8 January 2025, Published 28 March 2025

Keywords

anti COVID-19; antioxidant; molecular docking; *Premna serratifolia*; UHPLC-Q-Orbitrap HRMS.

ABSTRACT. This research aims to profile the active antioxidant compounds from leaf extracts of Buas-buas (*Premna serratifolia*) growing in Pontianak of West Kalimantan (Indonesia) through a metabolomics approach and their activity as anti-COVID-19 candidates by molecular docking. In this study, *P. serratifolia* leaves were macerated and fractionated using solvents with different polarities. The extracts were then tested for antioxidant activity using the DPPH method, determined the total phenolic content (TPC), flavonoids (TFC), and steroids (TSC), and analyzed antioxidant the functional groups and compounds by Fourier Transform Infrared spectroscopy (FTIR) and Ultra High-Performance Chromatography UHPLC-Q-Orbitrap HRMS. The functional groups on antioxidant activity were determined by Principal Component Analysis (PCA) and Partial Least Square (PLS) regression. Based on a metabolomics approach, the PCA and PLS analysis shows that hydroxyl was the most active antioxidant from *P. serratifolia* leaves. UHPLC-Q-Orbitrap HRMS analysis showed the presence of scopoletin, esculetin, 7-hydroxycoumarine, matairesinol, hymecromone, and hexylresorcinol in the water fraction of *P. serratifolia* leaves. Molecular docking with 4YE6, 1OG5, and 3NRZ shows that matairesinol had the most potential as an antioxidant. *Mataresinol* and hexyresorcinol are phenolic compounds that have great potential as a COVID-19 inhibitor based on molecular docking with 5R81, 7CMD, and 6M2N.

INTRODUCTION

The World Health Organization (WHO) confirmed in December 2023 that there were more than 772 million cases of COVID-19 in the world, including nearly 6.98 million deaths (WHO, 2023). COVID-19 will accelerate the reaction of free radicals in the body, causing respiratory syndrome (Flora *et al*., 2021). The antioxidant compounds in the medical plant, including *Premna serratifolia* can decrease the reactive oxygen species (ROS). *P. serratifolia* leaves, locally known as Buas-buas leaves by native West Borneo, extracted with ethanol by maceration and reflux methods have proven as an antioxidant (Isnindar *et al*., 2016; Lubaina *et al*., 2016; Purwanti *et al*., 2018; Puspita *et al*., 2020, Selvam *et al*., 2012; Simamora *et al*., 2020; Timotius *et al*., 2018). Flavonoids and phenolics in ethanol extract are predicted as important secondary metabolites in antioxidant activity. Identified by Liquid Chromatography-Quadrupole-Time of Flight-Mass Spectrometry/Mass Spectrometry (LC-QTOF-MS/MS), ethanol extract contains phenolic compounds, phylethanois, and flavonoid derivatives such as isoacteoside, scroside E, campneoside I, nobilin D, forsythoside A dan B, diosmin, and lavandulifolioside (Simamora *et al*., 2020). Meanwhile, the major compounds conducted on ethanol extract as the most affected functional groups in antioxidant activity, which represented metabolites, have not been discovered.

Cite this as: Hadiarti, D., Qurbaniah, M., Setiawan, E., and Sugara, T. H., 2025. Implementation of FTIR-Based Fingerprint, Antioxidant Compounds Profiling by UHPLC-Q-Orbitrap HRMS, and Docking Study COVID-19 Inhibitor of Buas-Buas (*Premna serratifolia*) Leaf Extract from Pontianak Indonesia. *ALCHEMY Jurnal Penelitian Kimia*, 21(1), 149-161. https://dx.doi.org/10.20961/alchemy.21.1.92020.149-161.

The determination of the functional groups that are most influential on antioxidants can be performed by a metabolomic approach using Fourier Transform Infrared (FTIR). This technique has been applied to understand the functional groups of the extract on robusta and arabica coffee (Kurniawan *et al*., 2017), *Syzygium polyanthum* (Rohaeti *et al*., 2020), as well as *Curculigo orchioides* and *C. latifolia* (Umar *et al*., 2021) which possibly decrease the free radical concentration. Furthermore, Analysis of Principal Component Analysis (PCA) and Partial Least Square (PLS) regression on the FTIR spectra study will also possibly show the primally functional groups on *P. serratifolia* affected antioxidant activity.

The identification utilizing LC-QTOF-MS/MS generally successfully identifies only eight antioxidant compounds from *P. serratifolia*. The separation and identification of the number of bioactive compounds in *P. serratifolia* will be increased by the separation and identification utilizing Ultra High-Performance Chromatography (UHPLC) and Quadrupole coupled Orbitrap analyzer on High-Resolution Mass Spectroscopy (HRMS). The extensive profiling of antioxidant compounds can be performed by UHPLC-Q-Orbitrap HRMS, which identified 23 phenolics from *Cannabis sativa* (Izzo *et al*., 2020) and 13 norlignan, triterpene, phenolics and their glycosides from *C. orchioides* and *C. latifolia* extracts (Umar *et al*., 2021).

P. serratifolia leaf extract has demonstrated free radical scavenging; however, the binding modes of phenolic compounds and oxidative enzymes cannot be explained. The interaction on the most stable complex of phenolic-enzyme can be predicted and analyzed by docking research (Mahomoodally *et al*., 2019). The *in-silico* study using molecular docking has been successful in the identification of active compounds as antioxidants from the extract *Malva sylvestris* (Irfan *et al*., 2021), *Zinnia elegans* (Samy *et al*., 2022) and *Onosma bourgaei* dan *O. trachytricha* (Istifli, 2021).

Metabolomics studies have never been used to identify active compounds that can perform as antioxidants in *P. serratifolia* leaves, including profiling active antioxidant compounds using UHPLC-Q-Orbitrap HRMS. *In-silico* testing of antioxidant and anti-covid-19 activities has also never been carried out on the active compounds of *P. serratifolia* leaf extract, which has been successfully identified using molecular docking. Therefore, as the evolution of COVID-19 cases increases, studying active compounds contained in *P. serratifolia* leaf extract is necessary to find the antioxidants that can slow down oxidation caused by free radicals and their inhibitory candidates.

MATERIALS AND METHODS

Plant Material, Extraction, and Fractionation

The leaves of *P. serratifolia* were collected in August 2020 in the peat forest in Pontianak of West Kalimantan, and a botanist at BRIN confirmed the plant taxonomy. The leaves were dried for 7 days and mashed using a blender. The resulting leaves powder was macerated in ethanol for 3 × 24 hours and fractioned by different polarity solvents such as hexane, ethyl acetate, and water (Hadiarti *et al*., 2021).

Determination of Total Flavonoids, Phenolics, and Steroids

The total flavonoid content (TFC), total phenolic content (TPC), and total steroid content (TSC) were determined by the $AlCl_3$, Folin-Ciocalteu, and Liebermann-Burchard methods utilizing quercetin, gallic acid, and cholesterin as standards. The UV-Vis spectrophotometer was used to measure the absorbance of standards (quercetin, gallic acid, and cholesterin) and samples (extract/fraction) at 725, 752, and 420 nm. Results of TFC, TPC, and TSC were expressed as grams standard equivalents per gram of sample (Hadiarti *et al*., 2021).

Antioxidant Test by DPPH Method

Antioxidant activity tests were carried out by combining the 1,1-diphenyl-1-picrylhydrazyl (DPPH) method used in research (Castaldo *et al*., 2020; Izzo *et al*., 2020; Umar *et al*., 2021). DPPH standard solution was prepared by dissolving 4 mg in 10 mL of ethanol and measuring the absorbance at a wavelength of 517 nm. Furthermore, 100 µL of *P. serratifolia* extract solution was added to 0.5 mL of DPPH solution. The mixture was then incubated at 37 °C for 30 min, and the absorbance was measured at 517 nm with a UV-Vis spectrophotometer. The results were further analyzed to obtain the value of IC_{50}.

The Analysis of FTIR

The FTIR analysis using Shimadzu IRPrestige-21 (Tokyo, Japan) was conducted by homogenizing 2 mg of *P. serratifolia* extract/fraction with 180 mg of KBr. Subsequently, the formed mixture was compressed into pellets under a pressure of 8 tons for 15 minutes. Following this step, the pellets were analyzed three times for each extract using the Shimadzu IRPrestige-21 FTIR spectrometer (Tokyo, Japan) in the wavelength range of 4000 – 400 cm^{-1} with a resolution of 4 cm^{-1}, yielding spectra with a scan rate of 45 scans per minute (Hadiarti *et al*., 2021).

Identification of Antioxidant Compounds using UHPLC-Q-Orbitrap HRMS

The chromatographic separation of compounds from water extract of *P. serratifolia* leaves was performed on the UHPLC-Q-Orbitrap HRMS with an AccucoreTM Phenyl Hexyl separation column (100 × 2.1 mm, 2.6 µm). Eluent A (formic acid in water) and eluent B (formic acid in acetonitrile) were used as mobile phase and flowed gradient starting from 5% B, increased to 95% in 25 min, stayed 95% B in 28 min, and decreased concentration B to 5% to 30 min. The mobile phase flow rate was set at 0.25 mL/min, and the injection volume was 5 µL. The qualitative identification of bioactive compounds was detected by a High-Resolution Mass Spectrometer using Q Exactive and Orbitrap analyzer operating in Electron Spray Ionization (ESI^+ and ESI^-) mode. The Compound Discover version 2.2 was processed to interpret UHPLC-Q-Orbitrap HRMS results (Castaldo *et al*., 2021; Hadiarti *et al*., 2023; Umar *et al*., 2021).

Molecular Docking Procedure

The crystal structure oxidants (4EY6, 1OG5, and 3NRZ) and COVID-19 (5R81, 7CMD, and 6M2N) enzymes were downloaded from the RSCB Protein Data Bank. The 3-D structures of identified phenolic compounds from *P. serratifolia* were obtained from the PubChem website in SDF format and then converted into PDB format using Open Bable GUI v2.3 software. The Chimera (Version 1.14) was operated to prepare phenolic compounds and proteins before docking to predict the binding modes of antioxidants and phenolics utilizing AutoDock Tools v1.5.6. The size of the grid box in macromolecules was set at 40 × 40 × 40 Å and grid spacing of 0.375 Å. The molecular docking simulation was performed using Autodock 4.2, and the Lamarckian Genetic Algorithm was employed with 100 runs, 2.500.000 energy evaluations, and a population size of 150. The Biovia Discovery Studio Visualizer 2021 software was operated to visualize the hydrophilic and hydrophobic interaction between the phenolics and proteins (Barros *et al*., 2018; Hadiarti *et al*., 2023; Istifli, 2021).

Statistical Analysis

The differences of TFC, TPC, TSC, IC_{50}, and inhibition concentration data were evaluated by one-way ANOVA and Tukey assay with a level of significance at 0.05 using XLSAT 5.03 statistical software. The PCA and PLS analyses were performed to evaluate the influence of the functional groups on antioxidant activity. All statistical analysis steps were finished according to our previous research (Hadiarti *et al*., 2021).

RESULT AND DISCUSSION

The powder of *P. serratifolia* leaves was macerated with ethanol and fractioned by using different polarities of solvents. The highest TFC and TPC resulted in water fraction, which means that most flavonoids and phenolics in *P. serratifolia* leaves are polar (Table 1). The antioxidant activity was expressed by the capability of extracts of *P. serratifolia* leaves to reduce 50% of free radical scavengers (IC_{50}) in Table 1. The water fraction had the strongest antioxidant activity. Compared to the previously reported, the IC_{50} value of water fraction in the present study was lower than (Simamora *et al*., 2020) (66.83 ± 1.14 µg/mL), and it is predicted because of the higher TPC (8.088 times).

Table 1. Total flavonoids, phenolics, and steroids content with antioxidant activity of *P. serratifolia* extracts.

Extract/ fraction	TFC (g QE/g extract)	TPC (g GAE/g extract)	TSC (g CE/g extract)	Antioxidant Activity (IC_{50}, µg/mL extract)	Inhibition at concentration of 20 µg/mL (%)
Ethanol	2.36 ± 0.92^{c}	10.82 ± 0.62^{b}	0.81 ± 0.02^{c}	63.49 ± 0.28^{a}	39.02 ± 0.05^{a}
Hexane	6.34 ± 0.90^{a}	5.99 ± 0.12^{c}	1.70 ± 0.15^{a}	nd	19.89 ± 0.73^{d}
Ethyl acetate	6.11 ± 0.72^{b}	6.66 ± 0.16^{c}	1.49 ± 0.26^{b}	59.14 ± 0.05^{b}	21.19 ± 0.04^{a}
Water	6.56 ± 0.15^{d}	21.84 ± 0.07^{a}	0.89 ± 0.12^{c}	35.95 ± 0.10^{c}	4.91 ± 0.36^{c}

Notations: Results were taken from triplicate tests represent the mean ± SD. The a-d letters indicate the grouping of the significant differences for each sample using his Tukey assay. Notation of nd means not determined.

The effect of the functional groups in *P. serratifolia* leaves extract (listed in Table 2) on antioxidant activity was conducted and analyzed by multivariant data analysis through PCA and PLS.

Table 2. The functional groups of *P. Serratifolia* extract identified from FTIR spectra presented in Figure SI-1.

Peak Code	Wavenumber (cm^{-1})	Functional Groups	Vibration Mode
A	3603.028	O–H	Stretching
B	2947.231	C–H	Stretching
C	2368.586	O=C=O, N–H	Stretching
D	2345.440	O=C=O	Stretching
E	1681.927	C=O	Stretching
F	1527.622	C=C (aromatic)	Stretching
G	1473.615	O–H	Bending
H	1419.608	CH (CH_3)	Bending
I	1381.032	C–O	Bending
J	1265.303	C–O (OH, COOH)	Bending
K	1165.005	C–C	Bending
L	1110.998	C–O	Stretching (aliphatic of ether)
M	1080.137	C–O	Stretching (secondary alcohol)
N	933.547	C–H (alkene)	Bending (trans disubtituen)
O	871.825	C–H (aromatic)	Bending
P	817.818	C–H (aromatic)	Bending (trisuntituen)
Q	786.957	C–Cl	Bending
R	671.228	C–X (halogen)	Halogen and aromatic disubtituen

On the PCA score plot (Figure 1), an obvious separation among the different extracts and metabolites can be seen, with an appropriate total variance of 80% of Principal Component-1 (PC-1) and 15% of Principal Component-2 (PC-2). The PCA biplot of *P. serratifolia* leaves extract exhibited that the hexane fraction was separated from other fractions according to the polarity of solvent extraction. The ethanol, ethyl acetate, and water fractions are distributed in the close area on the score plot, which indicates the similarity of functional group contents but different intensities. The water and hexane fractions are clustered on the positive side of PC1, while the ethyl acetate and ethanol fractions are located on the negative side. Although the water and hexane fractions are both on the positive side of PC1, they are positioned on opposite sides of PC2. This indicates differences in the polarity of the fractions, with water being polar and hexane being non-polar.

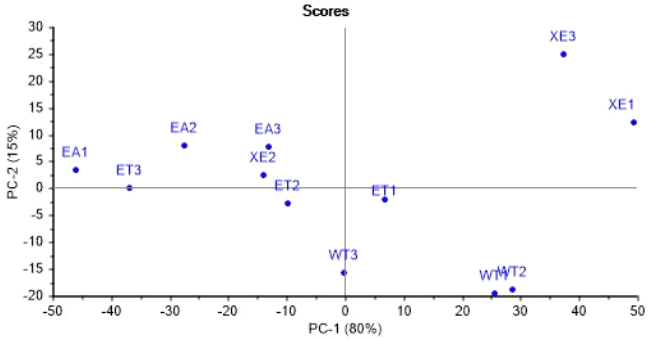

Figure 1. PCA biplot for primary components (PC-1) and (PC-2) of *P. serratifolia* leaves extract.

The bioactivity was studied using a PLS biplot, which combines score and loading plots. The distance between the X and Y variables and the sample clusters reflects the degree of their contribution to each respective cluster's characteristics. The strength contribution of the hydroxyl to affect antioxidant activity compared to other functional groups was emphasized by the PLS plot in Figure 2. In line with the previous research, the free radical oxidative stress could be influenced by OH, C–H aromatic, C=O, C=C, and C–O groups on phenolic compounds (Rohaeti *et al*., 2020; Umar *et al*., 2021). The hydroxyl groups presenting the phenolic compounds showed the strongest correlation with the DPPH scavenging activity of *Neptunia oleracea* (Lee *et al*., 2019), *Ziziphus mauritiana*, *Ziziphus spina-christi*, and *Ziziphus jujuba* (Sakna *et al*., 2019), *Malva sylvestris* (Irfan *et al*., 2021), *Asphodeline taurica* (Lazarova *et al*., 2019), *Hypericum lanuginosum* (Mahomoodally *et al*., 2019), *Salvia viridis* (Zengin *et al*., 2019), and *Asphodelus albus* (Lazarova *et al*., 2020). According to previous research findings, the hydroxyl groups in phenolic compounds from *P. serratifolia* leaf extract will likely play a significant role in antioxidant activity. This hypothesis can be validated by identifying compounds from the fraction with the highest antioxidant activity, followed by a molecular docking analysis of these identified compounds.

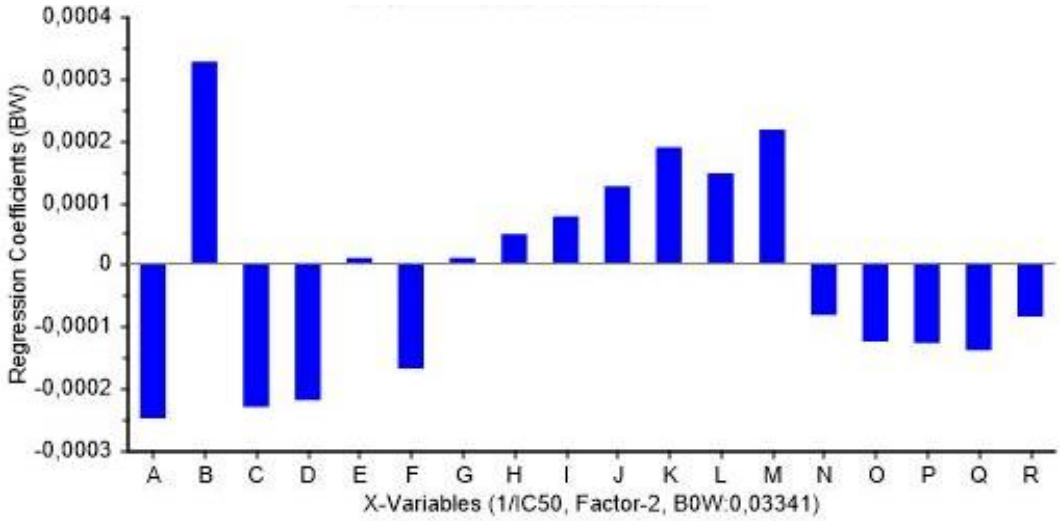

Figure 2. PLS plot as correlation of the functional groups and antioxidant extract of *P. serratifolia.*

The ESI^+ and ESI^- mode from UHPLC-Q-Orbitrap HRMS was operated to identify bioactive compounds of *P. serratifolia* water extract. The UHPLC-Q-Orbitrap HRMS spectra demonstrated the presence of six phenolics (scopoletin, 7-hydroxycoumarine, matairesinol, hymecromone, esculetin, and hexylresorcinol), nine flavonoids (kaempferide, centaureidin, glycitei, chyrsin, casticin, 3,5,4'-trimethoxy-6,7-methylenedioxyflavone, tricin, syringetin, and pectolinaringenin), and two uncategorized compounds (NP-018660 and NP-021797). The spectra interpretations in Table 3 are focused on phenolic compounds because of their highest correlation with antioxidant activity measured by PCA analysis and PLS regression through metabolomic approach. Compared to previous antioxidant studies, there is no similarity in identified phenolics between ours and the research reported by Simamora *et al*., 2020 and Timotius *et al*., 2018. *P. serratifolia* sources can differently influence bioactive phenolics since it depends on the growing location (Karimi *et al*., 2020; Wen *et al*., 2020), such as Central Sulawesi and West Kalimantan.

Table 3. Identified Phenolic Compounds in the *P. serratifolia* leaves extracts through UHPLC-Q-Orbitrap HRMS analysis.

Compound	PubChem ID	RT (min)	Molecular Formula	Adduct Ion	Theory Mass (*m/z*)	Experiment Mass (*m/z*)	Accuracy (ppm)
Scopoletin	5280460	7.92	$C_{10}H_8O_4$	$[M-H]^-$	192.04230	192.04286	3.13
Esculetin	5281416	8.89	$C_9H_6O_4$	$[M+H]^+$	178.02660	178.02561	-5.61
Hexylresorcinol	3610	11.84	$C_{12}H_{18}O_2$	$[M+H]^+$	194.13070	194.12979	-4.58
7-Hydroxycoumarine	5281426	12.07	$C_9H_6O_3$	$[M+H]^+$	162.03040	162.03074	2.40
Matairesinol	119205	12.36	$C_{20}H_{22}O_6$	$[M+H]^+$	358.14160	358.14004	-4.46
Hymecromone	5280567	15.33	$C_{10}H_8O_3$	$[M+H]^+$	176.04730	176.04658	-4.34

All identified phenolic compounds in Figure 3 have shown to have the potential to decrease the concentration of free radical oxidative stress. Isolated scopoletin from the bark of *Fagraea ceilanica* (Ferdinal *et al*., 2015) and the root of *Hypochaeris radicata* (Jamuna *et al*., 2015) was demonstrated as the antioxidant compound. Reduction of oxidative stress was performed by esculetin, which is isolated from *Cortex fraxini* (Wang *et al*., 2011) and identified from *Ipomoea batatas* (Shi *et al*., 2022). 7-hydroxycoumarine from extract *Lonicera Quinquelocularis*, *Aegle marmelos*, and *Murraya koenigii* exhibited DPPH scavenging activity (Ali *et al*., 2013; Ng *et al*., 2018). Hexylresorcinol, identified in *Olea europaea* wood extract, demonstrated antioxidant activity. Detected hymecromone from *Aegialitis rotundifolia* ethanol leaves extract showed DPPH radical scavenging activity (Ghosh *et al*., 2019). Mataresinol was isolated from the methanolic extract of Austrocedrus chilensis wood and evaluated as having antioxidant properties (Donoso-Fierro *et al*., 2009).

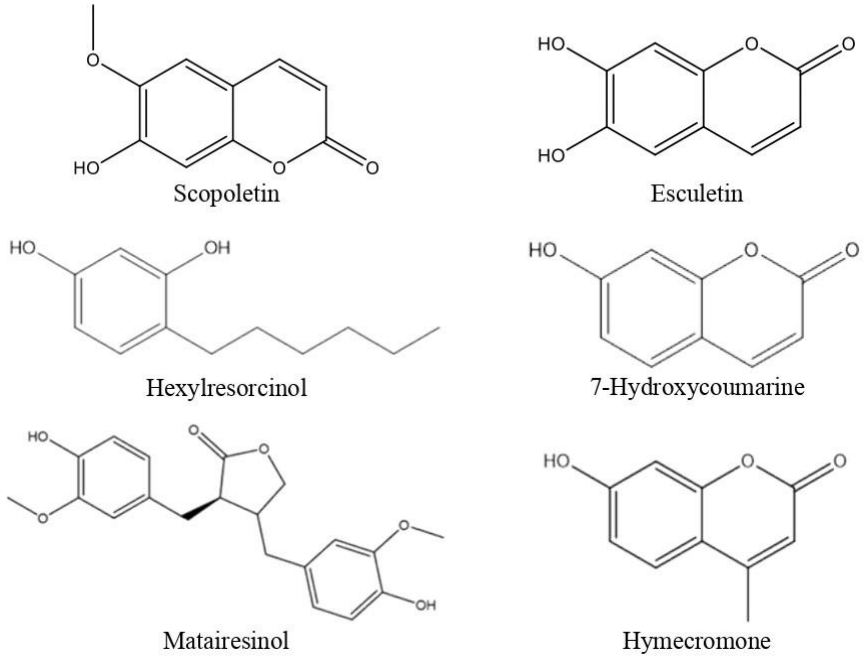

Figure 3. Structure of phenolic compounds water extract *P. serratifolia* leaves from UHPLC-Q-Orbitrap HRMS analysis.

The exploration of protein-ligand interaction has been studied to better understand the reduction mechanism of enzyme performance by identifying phenolics based on the best energy. Interaction of three oxidant enzymes, i.e., recombinant human acetylcholinesterase (PDB: 4EY6), human cytochrome (PDB: 1OG5), and bovine xanthine oxidase (PDB: 3NRZ) with six identified phenolics was accomplished by molecular docking. Based on the result in Table 4, matairesinol has binding energy and inhibitory constant lower than ascorbic acid as a control ligan. On the other hand, matairesinol has a significant antioxidant effect on *P. serratifolia*. According to the literature review, the interaction between 4EY6, 1OG5, and 3NRZ with matairesinol is computed for the first time.

Table 4. Binding energy, inhibitory constant (K_i), and hydrogen bond with free radical enzymes.

Compounds	Protein	$\Delta G_{binding}$ (kcal/mol)	K_i (μM)	Hydrogen Bond
Galanthamine (native ligan)	4EY6	-8.39	0.7084	TYR337, SER203, GLU202
S-Walfarin (native ligan)	1OG5	-7.85	1.76	ALA103, PHE100
Hypoxanthine (native ligan)	3NRZ	-5.39	112.80	GLU802, ARG880, THR1010
Ascorbic acid (control ligan)	4EY6	-3.83	157000	**GLU202**, GLY121, and GLY122
	1OG5	-2.63	1191000	**PHE100, ALA103**, ASN217, and GLN214
	3NRZ	-5.30	129.71	**THR1010**, **ARG880**, GLU1261, ALA1079, and **GLU802**
Scopoletin	4EY6	-5.01	214.36	ARG296 and **TYR337**
	1OG5	-4.57	449.81	GLN214 and **PHE100**
	3NRZ	-7.12	6.08	ALA1079, GLU1261, VAL1011, and **THR1010**
Esculetin	4EY6	-4.69	366.86	GLY120, TYR133, and **GLU202**
	1OG5	-4.37	628.38	ASN474 and **ALA103**
	3NRZ	-7.00	7.37	ALA1079, GLU1261, VAL1011, and **THR1010**
7-Hydroxycoumarine	4EY6	-4.59	428.76	ALA127, TYR133, and **GLU202**
	1OG5	-4.28	733.33	**ALA103**, LEU102, GLN214, and LEU208
	3NRZ	-6.28	24.90	GLU1261, VAL1011 and **THR1010**
Matairesinol	4EY6	-7.45	3.48	**GLU202**, GLY120, **SER203**, GLY12, and TYR124
	1OG5	-6.43	19.42	GLY98, **PHE100, ALA103,** and ASN217
	3NRZ	-7.12	5.99	ASN768 and **GLU802**
Hymecromone	4EY6	-5.08	190.08	ALA127, TYR133, and **GLU202**
	1OG5	-4.94	239.16	**ALA103**, LEU102, LEU208, and ASN217
	3NRZ	-6.21	27.89	ARG880 and **THR1010**
Hexylresorcinol	4EY6	-5.81	54.74	**GLU202**, GLY122, and **SER203**
	1OG5	-4.86	274.24	**PHE100** and GLY98
	3NRZ	-6.73	11.63	**GLU802** and SER1008

Notations: the terms in bold indicate hydrogen bonding interactions are the same as those of the native ligand.

Complex 4YE6-matairesinol was stabilized by two hydrogen bonds to GLU202 and SER203, as presented in Figure 4. Because these interactions had also occurred in galanthamine and hexylresorcinol with 4EY6 complex, as the second best of binding energy on identified phenolic and native ligan; those two residues are particularly essential being acetylcholinesterase enzyme. Unfavorable door-donor interaction indicates the repulsion of ALA204 with hydrogen atoms from 4EY6, which can reduce the stability of the 4YE6-matairesinol complex. GLU802 and THR1010 residues on hydrogen bonds play an important role in interaction with hypoxanthine enzymes. Phenolic compounds such as matairesinol and scopoletin, which have the best binding energy, interacted with these residues on 3NRZ through hydrogen bonds. Unfortunately, the principal hydrogen bond on 1OG5 can not be determined in this research.

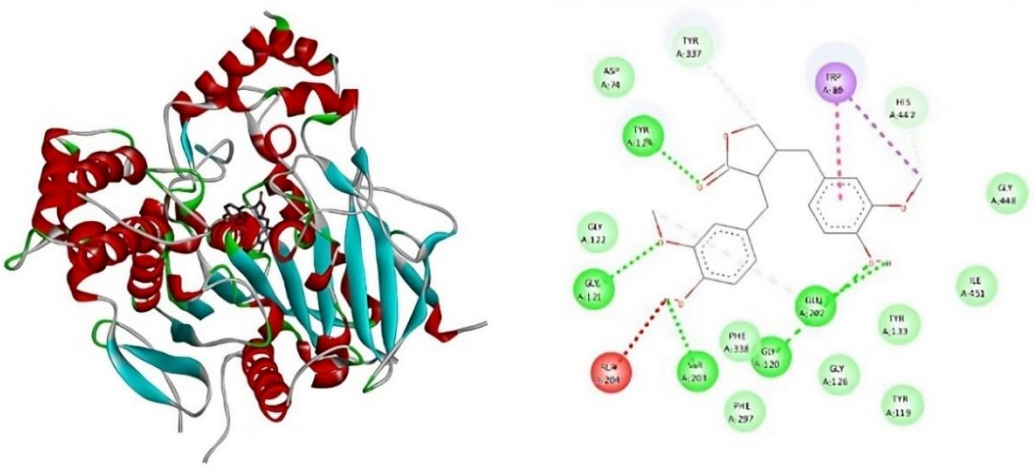

Interaction of *matairesinol* and 4EY6

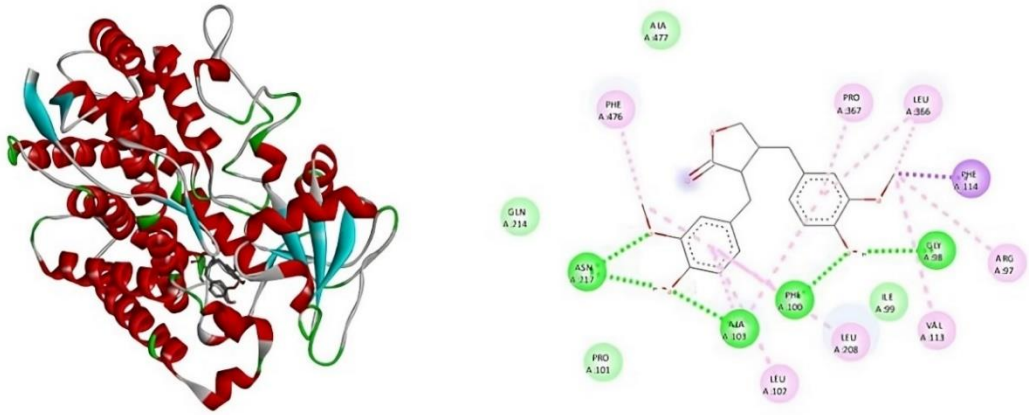

Interaction of *matairesinol* and 1OG5

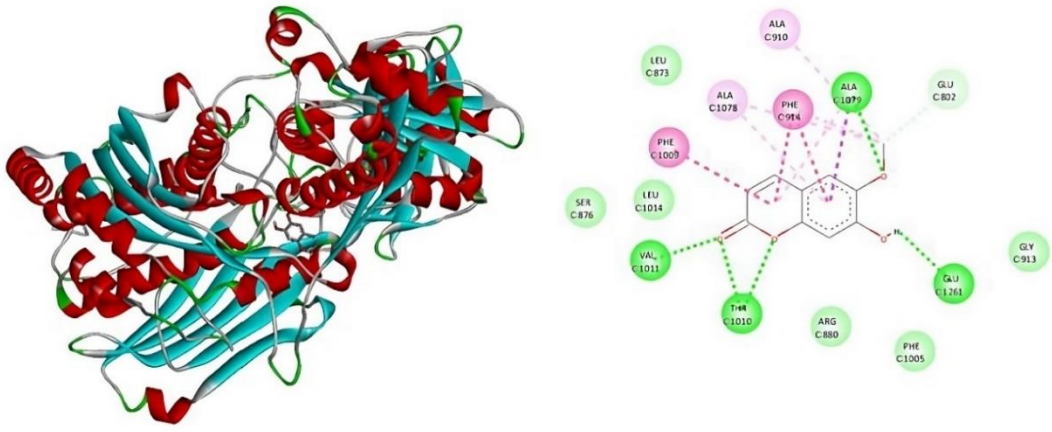

Interaction of *scopoletin* and 3NRZ

Figure 4. The 3D and 2D diagrams present the interaction of phenolics as potential antioxidants with 4YE6, 1OG5, and 3NRZ.

The prediction of antioxidant activity from *P. serratifolia* phenolic compounds that could be related to anti-COVID-19 was determined by molecular docking. In the current study, molecular research was accomplished for six phenolic compounds against 3 COVID-19 enzymes, including main protease (Mpro, PDB: 5R81), papain-like protease (PL pro, PDB: 7CMD), and 3CL protease (3CL pro, PDB; 6M2N). The lower binding energy than native and control ligan was performed by matariresinol and hexylresorcinol, so these phenolic compounds are potential

COVID-19 inhibitors from *P. serratifolia* (Table 5). No paper has been reported in a *silico* study through molecular docking between 5R81, 7CMD, and 6M2N with matairesinol and hexylresorcinol.

Tabel 5. Binding energy, inhibitory constant (K_i), and hydrogen bond with COVID-19 enzymes.

Compounds	Protein	$\Delta G_{binding}$ (kcal/mol)	K_i (μM)	Hydrogen Bond
1-methyl-3,4-dihydro-2~{H}-quinoline-7-sulfonamide (Native ligan)	5R81	-3.35	3529	GLU166
5-amino-2-methyl-N-[(1R)-1-naphthalen-1-ylethyl]benzamide (Native ligan)	7CMD	-8.15	1.05	GLN269, ASP164, and TRY268
5,6,7-trihydroxy-2-phenyl-4H-chromen-4-one (Native ligan)	6M2N	-6.00	39.84	GLU166 and LEU141
Asam askorbat (Control ligan)	5R81	-2.58	1284	**GLU166**, ARG188, THR190, GLN192, and VAL186
	7CMD	-4.56	452.74	SER245, ARG166, and **ASP164**
	6M2N	-4.16	898.00	**GLU166**, GLN189, ARG188, THR190, and GLN192
Scopoletin	5R81	-4.36	635.86	**GLU166,** GLN 192, dan THR190
	7CMD	-4.50	503.20	TYR273 and **GLN269**
	6M2N	-4.64	396.10	**GLU166**, GLN189, and GLY143
Esculetin	5R81	-3.90	1390	**GLU166** and PHE140
	7CMD	-4.16	897.71	**ASP164** and **TYR268**
	6M2N	-4.84	284.08	**GLU166** and SER144
7-Hydroxycoumarine	5R81	-4.29	711.76	**GLU166** and THR190
	7CMD	-4.12	951.56	**GLN269** and LEU163
	6M2N	-4.46	539.42	**GLU166** and SER144
Matairesinol	5R81	-5.06	194.53	**GLU166,** CYS145, dan LEU141
	7CMD	-8.41	0.69	ARG166, **ASP164**, and **GLN269**
	6M2N	-6.95	7.99	**GLU166**, GLY143, CYS145, **LEU141**, and GLN1189
Hymecromone	5R81	-4.26	755.26	**GLU166** and ARG188
	7CMD	-4.41	585.74	**GLN269**
	6M2N	-4.67	631.80	**GLU166**, CYS145, and GLY143
Hexylresorcinol	5R81	-5.10	181.48	**GLU166** and THR190
	7CMD	-5.28	133.95	**ASP164** and **GLN269**
	6M2N	-4.43	561.70	**GLU166** and GLN189

Notations: the bold term means hydrogen bonding interactions are the same as those of the native ligand.

As shown in Figure 5, one hydrogen bond stabilized the interaction between the GLU166 residue of the main protease enzyme and hexylresorcinol. The principal hydrogen bonds in papain-like protease are interactions on

ASP164 and GLN269 residues, which are demonstrated in a complex between 7CMD and native ligan and matairesinol. GLU166 and LEU141 on the 3CL protease enzyme have an important role, which is stabilizing the interaction between 6M2N and matairesinol.

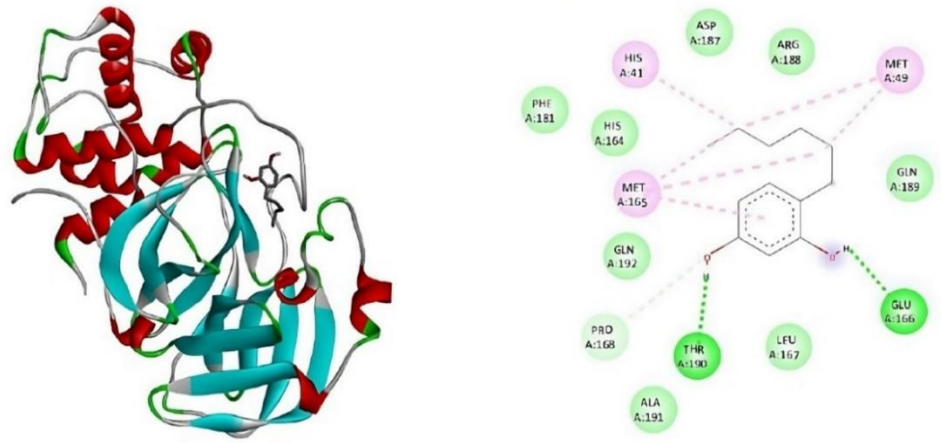

Interaction of *hexylresorcinol* and 5R81

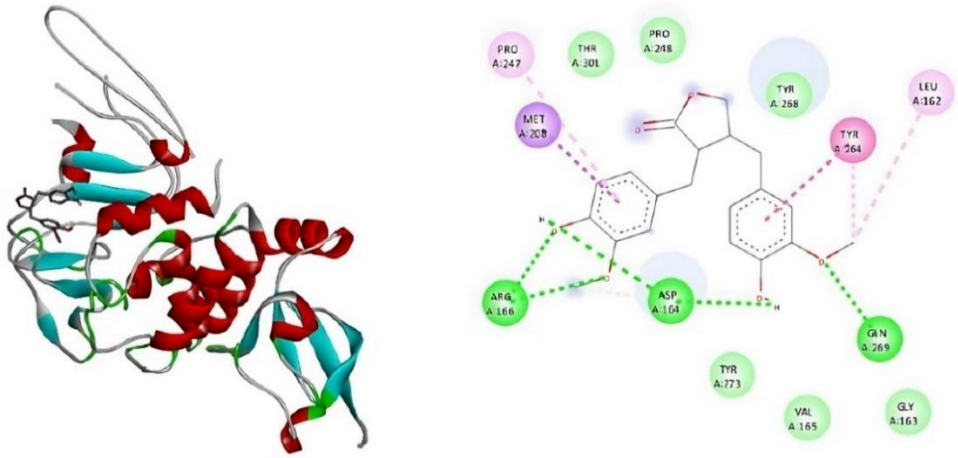

Interaction of *matairesinol* and 7CMD

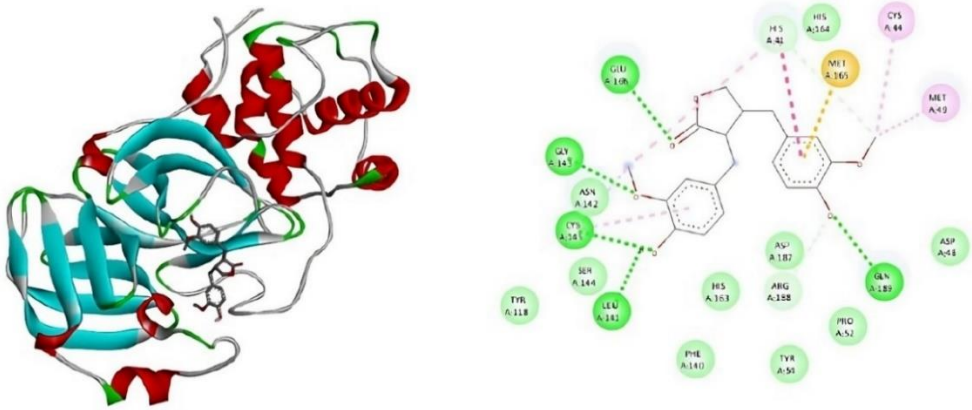

Interaction of *matairesinol* and 6M2N

Figure 5. The 3D and 2D diagrams present the interaction of phenolics as a potential antioxidants with 5R81, 7CMD, and 6M2N.

CONCLUSIONS

The water fraction of *P. serratifolia* leaves exhibited as the strongest antioxidant activity in the present study. Using metabolomic approach through PCA and PLS analysis, the results show that the hydroxyl group is a

principal compound in lowering free radical oxidative. Water fraction, which contains scopoletin, esculetin, 7-hydroxycoumarine, matairesinol, hymecromone, and hexylresorcinol, was identified by UHPLC-Q-Orbitrap HRMS. Based on a molecular docking study, matairesinol is the potential antioxidant, while the prospective anti-COVID-19 is hexylresorcinol and matairesinol. All complexes with the best binding energy between phenolic compounds with oxidant contained in *P. serratifolia* and COVID-19 proteins are reported for the first time in this study.

SUPPLEMENTARY INFORMATION

Figure SI-1 is available in supplementary information (SI) and accessible at https://jurnal.uns.ac.id/alchemy/rt/suppFiles/92020/0.

CONFLICT OF INTEREST

There is no conflict of interest in this article.

AUTHOR CONTRIBUTION

DH: Conceptualization, Methodology, Software; MQ: Data Analysis, Manuscript Drafting; ES: Supervision; THS: Manuscript Review and Editing.

ACKNOWLEDGEMENT

Thanks to the LPPM of the Muhammadiyah University of Pontianak for funding the research. Special thanks to the head of Biofarmaka and the IPB University Advanced Research Laboratory for facilitating the *in vitro* testing and analysis using the UHPLC-Q-Orbitrap HRMS.

DAFTAR PUSTAKA

Ali, I., Khan, D., Ali, F., Bibi, H., and Malik, A., 2013. Phytochemical, Antioxidant and Antifungal Studies on the Constituents of Lonicera Quinquelocularis. *Journal of the Chemical Society of Pakistan*, 35, 139–143.

Barros, S., Henrique, C., and Paula, T. De, 2018. An In Silico Study of the Antioxidant Ability for Two Quantum Chemical Methods. *Molecules*, 23, 1–17. https://doi.org/10.3390/molecules23112801.

Castaldo, L., Izzo, L., De Pascale, S., Narváez, A., Rodriguez-Carrasco, Y., and Ritieni, A., 2021. Chemical Composition, in Vitro Bioaccessibility and Antioxidant Activity of Polyphenolic Compounds from Nutraceutical Fennel Waste Extract. *Molecules*, 26, 1–12. https://doi.org/10.3390/molecules26071968.

Castaldo, L., Narváez, A., Izzo, L., Graziani, G., and Ritieni, A., 2020. In Vitro Bioaccessibility and Antioxidant Activity of Coffee Silverskin Polyphenolic Extract and Characterization of Bioactive Compounds Using UHPLC-Q-Orbitrap HRMS. *Molecules*, 25, 1–14. https://doi.org/10.3390/molecules25092132.

Donoso-Fierro, C., Becerra, J., Bustos-Concha, E., and Silva, M., 2009. Chelating and Antioxidant Activity of Lignans from Chilean Woods (Cupressaceae). *Holzforschung*, 63, 559–563. https://doi.org/10.1515/HF.2009.123.

Ferdinal, N., Alfajri, R., and Arifin, B., 2015. Isolation and Characterization of Scopoletin from the Bark of Fagraea Ceilanica Thumb and Antioxidants Tests. *International Journal on Advanced Science, Engineering and Information Technology*, 5, 126–130. https://doi.org/10.18517/ijaseit.5.2.504.

Flora, S.D., Balansky, R., and La Maestra, S., 2021. Antioxidants and COVID-19. *Journal of Preventive Medicine and Hygiene*, 62, E34–E45. https://doi.org/10.15167/2421-4248/jpmh2021.62.1S3.1895.

Ghosh, D., Mondal, S., and Ramakrishna, K., 2019. Phytochemical Profiling Using LC-Q-TOF-MS Analysis and In Vitro Antioxidant Activity of A Rare Salt-Secreting Mangrove *Aegialitis rotundifolia* Roxb. Leaves Extract. *International Journal of Pharmacy and Pharmaceutical Sciences*, 11, 37–47. https://dx.doi.org/10.22159/ijpps.2019v11i3.29985.

Hadiarti, D., Haryadi, W., Matsjeh, S., and Swasono, R.T., 2021. Understanding Phytochemical Roles on A-Glucosidase Inhibitory Activity Based on Metabolomic Approach of Premna Serratifolia Leaves from West Borneo, Indonesia. *Rasayan Journal of Chemistry*, 14, 1216–1222. https://doi.org/10.31788/rjc.2021.1426320.

Hadiarti, D., Haryadi, W., Matsjeh, S., Swasono, R.T., and Awaliyah, N., 2023. Profiling of α-Glucosidase Inhibitors from Ethyl Acetate Fraction of Buas-Buas (*Premna serratifolia*) Leaves Using UHPLC-Q-Orbitrap HRMS and Protein-Ligand Interaction with Molecular Docking. *Journal of Applied Pharmaceutical Science*, 13, 1–10. https://doi.org/10.7324/japs.2023.130210.

Irfan, A., Imran, M., Khalid, M., Sami Ullah, M., Khalid, N., Assiri, M.A., Thomas, R., Muthu, S., Raza Basra, M.A., Hussein, M., Al-Sehemi, A.G., and Shahzad, M., 2021. Phenolic and Flavonoid Contents in Malva Sylvestris and Exploration of Active Drugs as Antioxidant and Anti-COVID19 by Quantum Chemical and Molecular Docking Studies. *Journal of Saudi Chemical Society*, 25, 1–12. https://doi.org/10.1016/j.jscs.2021.101277.

Isnindar, Subagus, W., Widyarini, S., and Yuswanto, 2016. Determenation of Antioxidant Activities of Buas-Buas (*Premna serratifolia* L.) Using DPPH (2, 2-Diphenyl-1- Picrylhydrazyl) Method. *Traditional Medicine Journal*, 21, 111–115. https://doi.org/10.22146/tradmedj.17292.

Istifli, E.S., 2021. Chemical Composition, Antioxidant and Enzyme Inhibitory Activities of *Onosma bourgaei* and *Onosma trachytricha* and in Silico Molecular Docking Analysis of Dominant Compounds. *Molecules*, 26, 1–18. https://doi.org/10.3390/molecules26102981.

Izzo, L., Castaldo, L., Narváez, A., Graziani, G., Gaspari, A., Rodríguez-Carrasco, Y., and Ritieni, A., 2020. Analysis of Phenolic Compounds in Commercial *Cannabis sativa* L. Inflorescences Using UHPLC-Q-Orbitrap HRMs. *Molecules*, 25, 1–12. https://doi.org/10.3390/molecules25030631.

Jamuna, S., Karthika, K., Paulsamy, S., Thenmozhi, K., Kathiravan, S., and Venkatesh, R., 2015. Confertin and Scopoletin from Leaf and Root Extracts of *Hypochaeris radicata* Have Anti-Inflammatory and Antioxidant Activities. *Industrial Crops and Products*, 70, 221–230. https://doi.org/10.1016/j.indcrop.2015.03.039.

Karimi, A., Krähmer, A., Herwig, N., Schulz, H., Hadian, J., and Meiners, T., 2020. Variation of Secondary Metabolite Profile of *Zataria multiflora* Boiss. Populations Linked to Geographic, Climatic, and Edaphic Factors. *Frontiers in Plant Science*, 11, 1–15. https://doi.org/10.3389/fpls.2020.00969.

Kurniawan, M.F., Andarwulan, N., Wulandari, N., and Rafi, M., 2017. Metabolomic Approach for Understanding Phenolic Compounds and Melanoidin Roles on Antioxidant Activity of Indonesia Robusta and Arabica Coffee Extracts. *Food Science and Biotechnology*, 26, 1475–1480. https://doi.org/10.1007/s10068-017-0228-6.

Lazarova, I., Zengin, G., Gevrenova, R., Nedialkov, P., Aneva, I., Aumeeruddy, M.Z., and Mahomoodally, M.F., 2019. A Comparative Study of UHPLC/Orbitrap MS Metabolomics Profiles and Biological Properties of *Asphodeline taurica* from Bulgaria and Turkey. *Journal of Pharmaceutical and Biomedical Analysis*, 168, 174–180. https://doi.org/10.1016/j.jpba.2019.02.008.

Lazarova, I., Zengin, G., Sinan, K.I., Aneva, I., Uysal, S., Picot-Allain, M.C.N., Aktumsek, A., Bouyahya, A., and Mahomoodally, M.F., 2020. Metabolomics Profiling and Biological Properties of Root Extracts from Two Asphodelus Species: *A. Albus* and *A. Aestivus*. *Food Research International*, 134, 109277. https://doi.org/10.1016/j.foodres.2020.109277.

Lee, S.Y., Mediani, A., Ismail, I.S., Maulidiani, and Abas, F., 2019. Antioxidants and α-Glucosidase Inhibitors from *Neptunia oleracea* Fractions Using 1 H NMR-Based Metabolomics Approach and UHPLC-MS/MS Analysis 03 Chemical Sciences 0301 Analytical Chemistry. *BMC Complementary and Alternative Medicine*, 19, 1–15. https://doi.org/10.1186/s12906-018-2413-4.

Lubaina, A.S., Brijithlal, N.D., and Murungan, K., 2016. Phytochemical Analysis and Antioxidant Potentiality of *Premna serratifolia* L. an Aromatic Medicinal Plant. *World Journal Of Pharmaceutical Research*, 5, 841–852. https://doi.org/10.20959/wjpr201612-7439.

Mahomoodally, M.F., Zengin, G., Zheleva-Dimitrova, D., Mollica, A., Stefanucci, A., Sinan, K.I., and Aumeeruddy, M.Z., 2019. Metabolomics Profiling, Bio-Pharmaceutical Properties of *Hypericum lanuginosum* Extracts by In Vitro and In Silico Approaches. *Industrial Crops and Products*, 133, 373–382. https://doi.org/10.1016/j.indcrop.2019.03.033.

Ng, R.C., Kassim, N.K., Yeap, Y.S.Y., Lian Ee, G.C., Yazan, S.L., and Musa, K.H., 2018. Isolation of Carbazole Alkaloids and Coumarins from Aegle Marmelos and Murraya Koenigii and Their Antioxidant Properties. *Sains Malaysiana*, 47, 1749–1756. https://doi.org/10.17576/jsm-2018-4708-14.

Purwanti, N.U., Wahdiyanti, R., and Susanti, R., 2018. Effect of Variation of Solvent Concentration to Antioxidant Activity of Ethanolic Extract of Buas-Buas Stem (*Premna serratifolia* L.) Using DPPH (2, 2-Diphenyl-1 Picrylhidrazyl) Scavenging Method. *International Conference on Pharmaceutical Research and Practice*. ICPRP, 15-17 December 2018, Yogyakarta, pp. 126–132.

Puspita, W., Yuspita Sari, D., and Ristia Rahman, I., 2020. Uji Aktivitas Antioksidan Ekstrak Etanol Daun Buas-Buas (*Premna serratifolia* L.) Asal Kabupaten Melawi Provinsi Kalimantan Barat dengan Metode DPPH. *Jurnal Insan Farmasi Indonesia*, 3, 405–412. https://doi.org/10.36387/jifi.v3i2.532.

Rohaeti, E., Karunina, F., and Rafi, M., 2020. FTIR-Based Fingerprinting and Chemometrics for Rapid Investigation of Antioxidant Activity from *Syzygium polyanthum* Extracts. *Indonesian Journal of Chemistry*, 21, 128–136. https://doi.org/10.22146/ijc.54577.

Sakna, S.T., Mocan, A., Sultani, H.N., El-fiky, N.M., Wessjohann, L.A., and Farag, M.A., 2019. Metabolites Profiling of Ziziphus Leaf Taxa via UHPLC/PDA/ESI-MS in Relation to Their Biological Activities. *Food Chemistry*, 293, 233–246. https://doi.org/10.1016/j.foodchem.2019.04.097.

Samy, M.N., Gomaa, A.A.-R., Attia, E.Z., Ibrahim, M.A.A., Desoukey, S.Y., and Kamel, M.S., 2022. Flavonoids of Zinnia Elegans: Chemical Profile and, in Vitro Antioxidant and in Silico Anti-COVID-19 Activities. *South African Journal of Botany*, 147, 576–585. https://doi.org/10.1016/j.sajb.2022.02.024.

Selvam, T.N., Venkatakrishnan, V., Damodar Kumar, S., and Elumalai, P., 2012. Antioxidant and Tumor Cell Suppression Potential of *Premna serratifolia* Linn Leaf. *Toxicology International*, 19, 31–34. https://doi.org/10.4103/0971-6580.94514.

Shi, J., Wu, Q., Deng, J., Balfour, K., Chen, Z., Liu, Y., Kumar, S., Chen, Y., Zhu, Z., and Zhu, G., 2022. Metabolic Profiling and Antioxidant Analysis for the Juvenile Red Fading Leaves of Sweetpotato. *Plants*, 11, 1–15. https://doi.org/10.3390/plants11223014.

Simamora, A., Santoso, A.W., Timotius, K.H., and Rahayu, I., 2020. Antioxidant Activity, Enzyme Inhibition Potentials, and Phytochemical Profiling of Premna Serratifolia L. Leaf Extracts. *International Journal of Food Science*, 2020, 1–11. https://doi.org/10.1155/2020/3436940.

Timotius, K.H., Simamora, A., and Santoso, A.W., 2018. Chemical Characteristics and in Vitro Antidiabetic and Antioxidant Activities of *Premna serratifolia* L. Leaf Infusion and Decoction. *Pharmacognosy Journal*, 10, 1114–1118. https://doi.org/10.5530/pj.2018.6.189.

Umar, A.H., Ratnadewi, D., Rafi, M., and Sulistyaningsih, Y.C., 2021. Untargeted Metabolomics Analysis Using FTIR and UHPLC-Q-Orbitrap HRMS of Two Curculigo Species and Evaluation of Their Antioxidant and α-Glucosidase Inhibitory Activities. *Metabolites*, 11, 1–17. https://doi.org/10.3390/metabo11010042.

Wang, K., Zhang, Y., Ekunwe, S.I.N., Yi, X., Liu, X., Wang, H., and Pan, Y., 2011. Antioxidant Activity and Inhibition Effect on the Growth of Human Colon Carcinoma (HT-29) Cells of Esculetin from Cortex Fraxini. *Medicinal Chemistry Research*, 20, 968–974. https://doi.org/10.1007/s00044-010-9426-y.

Wen, B., Ren, S., Zhang, Y., Duan, Y., Shen, J., Zhu, X., Wang, Y., Ma, Y., Zou, Z., and Fang, W., 2020. Effects of Geographic Locations and Topographical Factors on Secondary Metabolites Distribution in Green Tea at a Regional Scale. *Food Control*, 110, 106979. https://doi.org/10.1016/j.foodcont.2019.106979.

World Health Organization, 2023. *WHO Coronavirus Disease (COVID-19) Dashboard with Vaccination Data | WHO Coronavirus (COVID-19) Dashboard with Vaccination Data*. *World Health Organization*. <https://covid19.who.int/%0Ahttps://covid19.who.int/%0Ahttps://covid19.who.int/region/searo/country/bd> (accessed December 31, 2023).

Zengin, G., Mahomoodally, F., Picot-Allain, C., Diuzheva, A., Jekő, J., Cziáky, Z., Cvetanović, A., Aktumsek, A., Zeković, Z., and Rengasamy, K.R.R., 2019. Metabolomic Profile of *Salvia viridis* L. Root Extracts Using HPLC–MS/MS Technique and Their Pharmacological Properties: A Comparative Study. *Industrial Crops and Products*, 131, 266–280. https://doi.org/10.1016/j.indcrop.2019.01.060.